

COB-2023-1425

ANALYSIS OF FUEL IN SURFACE HEAT EXCHANGERS FOR AIRCRAFT

Henrique Carreira Martins

Edemar Morsch Filho

São Paulo State University (Unesp), School of Engineering, Department of Aeronautical Engineering, Campus of São João da Boa Vista. Av. Profa. Isette Corrêa Fontão, 505 - Jardim das Flores, São João da Boa Vista - SP, 13876-750

henrique.c.martins@unesp.br; edemar.filho@unesp.br

Laio Oriel Seman

Federal University of Santa Catarina (UFSC), Technological Center, Department of Automation and Systems, Campus of Florianópolis. R. Eng. Agrônomo Andrei Cristian Ferreira, s/n - Trindade, Florianópolis - SC, 88040-900

laio@ieee.com

Abstract. *This study simulates the thermal management of modern commercial aircraft using integrated fuel and surface heat exchangers. Conventional thermal management in aircraft generally directs atmospheric air to its interior, promoting a drag increase. As a significant part of the fuel of a civil commercial aviation aircraft is in the wing, which in turn has a relatively large surface area, is exposed to airflow with speeds greater than 800 km/h and at a temperature of -56°C , there is a huge potential to exchange heat using the wing and the circulation of fuel inside it, as in a surface heat exchanger. In this case, the fuel can be used to absorb and transport the heat loads from the systems before being rejected. To evaluate it, a lumped numerical model is developed considering typical operation phases. Despite the model adopting simplifying provisions regarding the flow and imposed geometry, the results allow exploring different scenarios that may be useful for the preliminary design of an aircraft. The model developed in this study suggests that the surface heat exchanger model integrated with the fuel is a promising technique when certain altitude and fuel flow characteristics are met.*

Keywords: Heat transfer, airplane, fuel, heat exchanger.

1. INTRODUCTION

The challenge of providing adequate thermal management onboard modern commercial aircraft has grown significantly in recent years. This topic is the subject of several Research, Development, and Innovation (RD&I) projects. Consequently, the number of publications on this topic shows a significant growth trend, especially in the last 5 years (van Heerden *et al.*, 2022). The motivation for this scenario can be explained, in part, by the progressive and continuous electrification of new aircraft, as well as by the miniaturization of electronic components found in the various aircraft. In addition, the greater presence of composite materials in the primary and secondary aircraft structures introduces extra difficulties for heat dissipation compared to conventional alloys due to their lower diffusivity and anisotropic behavior.

In the article of Rosero *et al.* (2007), the authors state that the next generations of MEA aircraft (*More Electric Aircraft*), with a capacity of 300 passengers, will need approximately 1.6 MW of power for the electrical system. When considering an efficiency of 95%, the heat generated by this system alone would be around 80 kW, which confirms the need to improve the thermal management systems of aircraft.

On an aircraft, cabin pressure and temperature conditions are typically the responsibility of the *Environmental Control System* (ECS). Generally, conventional models direct atmospheric air into the aircraft through valves in the engines or through small openings in the fuselage/wing. Inevitably, this technique increases drag, which is detrimental to a more efficient operation (Schlabbe and Lienig, 2016). Therefore, the search for better performance of an aircraft also involves the design of thermal management in the face of its demands, without disregarding the safety aspects involved, which explains why industry and academia have been seeking to improve and develop new heat dissipation methods for aircraft, mainly for the next MEA generations.

In the context of thermal management of aircraft, an alternative pointed out is the use of fuel as a thermal transport element of systems that generate heat, such as the cooling of engine oil already used in high-performance military aircraft (Gray and Shayeson, 1973), or even using the fuel tank as a large heat sink. Roland and Rumpfkeil (2017) point out that cooling using aircraft fuel is an alternative that presents the differential of being a kind of passive thermal control system and, to some extent, of lower complexity when compared to other systems.

Even if new technologies are on board the aircraft of the future, the geometric characteristics we know today will be present in the new configurations. In commercial aircraft, these characteristics are limited to a cylindrical fuselage and

swept wings. Therefore, large surface areas will still be exposed to the atmosphere, mainly on the wings and fuselage, which, together with the low temperatures and high speeds present during flight, make them excellent heat sinks by external forced convection.

However, it should be remembered that the complete operation of an aircraft is more comprehensive, and the main existing steps include the phase with the plane parked on the finger, taxiing, takeoff, climb, cruise, descent, landing, and taxiing again. Therefore, the combination of low temperatures and high speeds, the best conditions from the point of view of convective heat transfer, appears only in the cruise flight phase. In contrast, the highest temperature and lowest speed are found in the taxiing phase and represent the worst convection scenario. Therefore, the cooling capacity through the wing and fuselage surfaces is dynamic throughout the aircraft's operation. Consequently, the performance of a surface heat exchanger based on an airplane's wing area, having integrated at the hot branch the fuel flow, is also affected and must be evaluated for all these conditions.

For years, fuel has been used as a heat sink for engine oil. In cases where fuel flow is not sufficient, such as during taxiing and landing, a recirculation pump is installed to maintain the necessary flow. The use of the aircraft's fuel as a cooling fluid for its systems makes it possible to reduce the weight of the aircraft, as well as reduce drag (by minimizing the need to extract air through the engine) and reduce maintenance with the replacement of different types of refrigerant fluids for the same aircraft. However, one of the challenges of using fuel integrated with thermal management is the need for careful temperature control so that the combustion temperature is not reached, which would jeopardize the safety of the operation. According to Kellermann *et al.* (2020a), the temperature limits for not reaching ignition usually vary between 448 K and 511 K.

The present work has as its main objective to analyze, through numerical models of low computational cost, the viability of a surface heat exchanger for aircraft, considering the integration of a fuel duct under the surface of the wing to dissipate the heat generated in aircraft systems.

2. METHODOLOGY

The present work was developed to analyze the feasibility of using fuel as a working fluid in surface heat exchangers integrated into the wings of an aircraft, to dissipate heat from the aircraft systems. To estimate the capacity of this heat exchanger, a mathematical model was created, based mainly on studies by Kellermann *et al.* (2020b) and Kellermann *et al.* (2020a). Through this model, it is possible to estimate how much heat is dissipated by the wing surface for different operating configurations.

2.1 Geometric model and discretization

This study focuses on the use of aircraft fuel as a surface heat exchanger branch located along a wing, as shown in Fig. 1. In this way, the heat from generic sources of the aircraft is transferred to the fuel flow \dot{m}_f , and this flows in a duct covering the half-wing in the direction of its span, from the root to the tip.

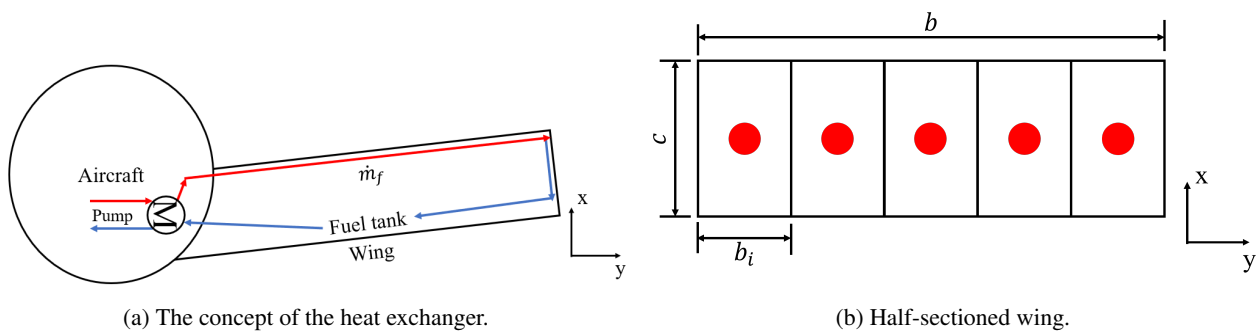


Figure 1: Geometric model and discretization.

To perform the calculations, the half-wing is divided into finite sections, and in each section there is a point (node), where the heat exchange and temperature are evaluated. Figure 1b illustrates the concept of this half-wing, where b is the span of the half-wing, c is the average aerodynamic chord of the half-wing and b_i is the length of each section. Each red dot represents a node, whose fuel temperature value to be calculated is representative of its entire respective section.

2.2 Energy conservation

In this section, the energy balance is performed to estimate the heat exchange capacity of the wing, with and without the passage of fuel inside it. First, the balance is performed without the fuel, in order to identify the potential for heat rejection through the wing surface. In a second moment, the fuel flow under the surface of the wing is introduced in the

model, with the objective of estimating its impact on heat transfer.

2.2.1 Wing as surface heat exchanger

According to Fig. 2 and considering only the steady state, the energy balance on the surface can be written by Eq. 1:

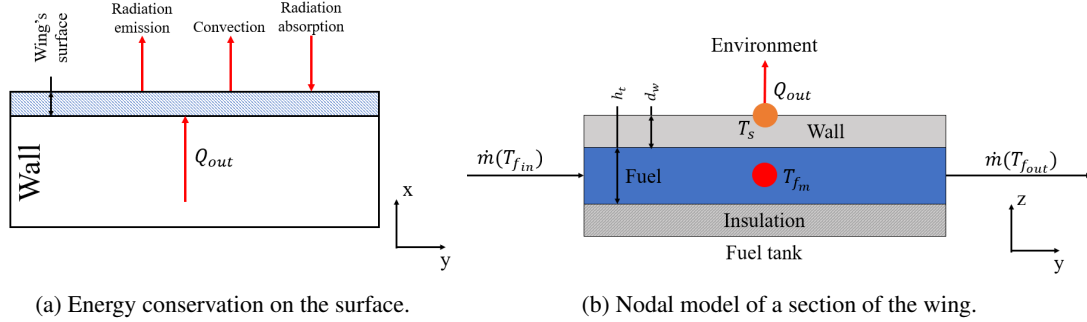


Figure 2: Thermal model.

$$Q_{out} = hA(T_s - T_{\infty}) + \varepsilon\sigma A(T_s^4 - T_{viz}^4) - \alpha A Q''_{sol} \quad (1)$$

where h is the convection heat transfer coefficient [W/m²K], A is the surface area [m²], T_s is the surface temperature [K], T_{∞} is the ambient temperature [K], ε is the emissivity [-], σ is the Stefan-Boltzmann constant [W/m² K⁴], T_{viz} is the temperature of the neighborhood [K], α the absorptivity [-] and Q''_{sol} is the solar radiation flux [W/m²]. The value obtained for Q_{out} is equivalent to the heat rejection through the surface, for that section.

2.2.2 Fuel in the hot branch of the heat exchanger

As shown in Fig. 2, the fuel enters with a mass flow rate (\dot{m}_f) [kg/s] at a temperature $T_{f_{in}}$ [K] on the left end, exchanges heat with the external environment through one of the faces, and exits with the same mass flow rate at a temperature $T_{f_{out}}$ [K] on the other side. This hot fuel flow transfers heat via internal forced convection, which is then conducted through the wall, leaving the external surface at temperature T_s [K], where it is then transferred to the air via external forced convection. The face opposite to the heat exchange is in contact with the fuel tank, whose capacity to exchange heat is much lower compared to external forced convection, so in this work it will be modeled as an adiabatic boundary condition.

Considering steady state, without internal energy generation and approximating the flow by a one-dimensional, incompressible flow, the energy balance in each section of the wing leads to:

$$\dot{m}c_p(T_{f_{in}} - T_{f_{out}}) = Q_{out} \quad (2)$$

where c_p is the specific heat of the fuel [J/kgK], and Q_{out} is the heat being withdrawn [W] through the surface.

Using the concept of thermal resistance:

$$Q_{out} = \frac{T_{f_m} - T_s}{R_h + R_k} \quad (3)$$

where T_{f_m} is the average temperature between the fuel inlet and outlet [K], R_h is the internal forced convection thermal resistance of the fuel and R_k is the thermal resistance of the flat wall.

Substituting Eq. 3 into Eq. 2:

$$\dot{m}c_p(T_{f_{in}} - T_{f_{out}}) = \frac{T_{f_m} - T_s}{R_h + R_k} \quad (4)$$

The average temperature of the fluid T_{f_m} , obtained at a position equidistant from the ends of the control volume, is:

$$T_{f_m} = \frac{T_{f_{in}} + T_{f_{out}}}{2} \quad (5)$$

Substituting this result in Eq. 4:

$$\dot{m}c_p (T_{f_{in}} - T_{f_{out}}) = \frac{0,5 (T_{f_{in}} + T_{f_{out}}) - T_s}{R_h + R_k} \quad (6)$$

Working in the equation:

$$T_{f_{out}} = \frac{T_{f_{in}} [\dot{m}c_p (R_h + R_k) - 0,5] + T_s}{[\dot{m}c_p (R_h + R_k) + 0,5]} \quad (7)$$

Using Eq. 3 and the definition of \dot{Q}_{out} given by Eq. 1:

$$hA (T_s - T_\infty) + \varepsilon\sigma A (T_s^4 - T_{viz}^4) - \alpha A Q''_{sol} = \frac{T_{f_m} - T_s}{R_h + R_k} \quad (8)$$

Substituting the definition of T_{f_m} and manipulating the equation:

$$T_{f_{in}} + T_{f_{out}} - 2T_s = 2 (R_{h_f} + R_k) \left[hA (T_s - T_\infty) + \varepsilon\sigma A (T_s^4 - T_{viz}^4) - \alpha A Q''_{sol} \right] \quad (9)$$

Substituting the equation of $T_{f_{out}}$ obtained in Eq. 7:

$$T_{f_{in}} + \frac{T_{f_{in}} [\dot{m}c_p (R_{h_f} + R_k) - 0,5] + T_s}{[\dot{m}c_p (R_{h_f} + R_k) + 0,5]} - 2T_s = 2 (R_{h_f} + R_k) A [h (T_s - T_\infty) + \varepsilon\sigma (T_s^4 - T_{viz}^4) - \alpha Q''_{sol}] \quad (10)$$

Therefore, providing the geometric parameters, materials, and other properties as a function of altitude, only the surface temperature T_s and the forced convection heat transfer coefficient h (internal and external) are unknown so far. The terms h can be estimated through relations involving the Nusselt number and will be presented in the next section. However, Eq. 10 is not linear and, therefore, in this work the Newton-Raphson method will be adopted to solve it. Once T_s is established, the exit temperature of the fuel $T_{f_{out}}$ is obtained through Eq. 7, as well as the heat transferred through the wing by integrating the fuel (Eq. 3).

2.3 Convective heat transfer coefficient

The coefficient of heat transfer by forced convection, whether internal or external flow, can be calculated by the dimensionless parameter known as the Nusselt number (Nu), thermal conductivity k [W/mK], and characteristic length L [m], according to the equation below (Cengel, 2008):

$$h = \frac{Nu k}{L} \quad (11)$$

2.3.1 External forced convection

In this case, the fluid involved in convection is atmospheric air and the geometry is the outer surface of the wing. For this work, it will be considered that the surface of the wing can be approximated by a flat plate, therefore the equation of the average Nusselt as a function of the chord c of the airfoil (Nu_c) will be (Cengel, 2008):

$$Nu_c = \left[0,664 Re_c^{1/2} + 0,037 \left(Re_c^{4/5} - Re_{cr}^{4/5} \right) \right] Pr^{1/3} \quad (12)$$

where Re_c is the Reynolds number based on the chord c and Pr is the Prandtl number of the fluid, both for air, and a widely accepted value for the critical Reynolds number is $Re_{cr} = 5 \times 10^5$.

2.3.2 Forced internal convection

In this case, the fluid involved in the internal forced convection used in this work will be aeronautical kerosene (JET-A). As for the geometry, a rectangular duct will be assumed that passes inside the wing, whose hydraulic diameter D_h is calculated by Eq. 13.

$$D_h = \frac{4l_t h_t}{2l_t + 2h_t} \quad (13)$$

To calculate the average Nusselt as a function of the hydraulic diameter D_h of the pipeline, the following expression will be used, valid only for turbulent flows with cooling Cengel (2008):

$$Nu_{D_h} = 0.023 Re_{D_h}^{0.8} Pr^{0.3} \quad (14)$$

where the Re_{D_h} and Pr of this equation are calculated based on the fuel flow. For all cases of internal flow it will be assumed that the flow is fully developed and the effects of the entrance region are negligible. The occurrence of a purely turbulent and fully developed flow is an assumption adopted to keep the model simple.

2.4 Thermal, surface and geometric properties

Table 1 presents some values used throughout the study for surface and geometry properties. The absorptivity, emissivity, thermal conductivity of the wall, and the flux of solar radiation were chosen according to the study of Kellermann *et al.* (2020a), while the others are stipulated by the present author.

Table 1: Parameters used in this study.

Parameter	Value
Absorptivity (α) [-]	0,25
Emissivity (ε) [-]	0,50
Thermal conductivity of the wall (k_w) [W/mK]	240
Height of the duct (h_t) [m]	0,015
Width of the duct (l_t) [m]	0,8c
Width of the wall (d_w) [m]	0,0015
Solar flux radiation (Q''_{sol}) [W/m ²]	1100

2.4.1 Thermal properties of the atmospheric air

The thermal properties of atmospheric air vary with temperature, which in turn varies with altitude (H [m]). The air parameters used in the work were calculated using the equations below:

- Temperature [K] (Binns, 2018):

$$T_\infty(H) = \begin{cases} 288,15 - (6,5 \times 10^{-3})H, & H \leq 11.000 \text{ m} \\ 216,65, & H > 11.000 \text{ m} \end{cases} \quad (15)$$

- Density [kg/m³] (Binns, 2018):

$$\rho_{ar}(T_\infty) = \begin{cases} 1,225 \times \left(\frac{T_\infty(H)}{288,15}\right)^{4.2523} & H \leq 11.000 \text{ m} \\ 0,3639 - 1,5758 \times 10^{-4}(H - 11.000) & H > 11.000 \text{ m} \end{cases} \quad (16)$$

- Dynamic viscosity [kg/ms] (Sadraey, 2017):

$$\mu_{ar}(T_\infty) = \frac{1,485\sqrt{T_\infty}}{1 + \left(\frac{110,4}{T_\infty}\right)} \times 10^{-6} \quad (17)$$

- Due to the small variation in relation to temperature, the specific heat of the air was considered constant and equal to $c_{p_{air}} = 1005$ J/kgK Cengel (2008).

- Thermal conductivity [W/mK] (Cengel, 2008):

$$k_{ar}(T_\infty) = 0,0198 + 7,5(T_\infty - 223) \times 10^{-5} \quad (18)$$

2.4.2 Thermal properties of the fuel

The fuel used in this work is aviation kerosene (JET-A), whose properties as a function of its temperature are presented below.

- Density [kg/m^3] (Bruno, 2008):

$$\rho_f = -0,0002T_{f_{in}}^2 - 0,6533T_{f_{in}} + 997,04 \quad (19)$$

- Dynamic viscosity [kg/ms] (Bruno, 2008):

$$\mu_f = (0,1862T_{f_{in}}^2 - 134,18T_{f_{in}} + 24720) \times 10^{-6} \quad (20)$$

- Specific heat [J/kgK] (Fortin and Bruno, 2022)

$$c_p = (0,004T_{f_{in}} + 0,7795) \times 10^3 \quad (21)$$

- Due to the small variation in relation to temperature, the thermal conductivity of the fuel was considered constant and equal to $k_f = 0,125 \text{ W/mK}$ (Bruno, 2008).

2.5 Cases of study: wing

In these cases, a total wing area of 200 m^2 was used, similar to what was observed in the work by Kellermann *et al.* (2020b).

2.5.1 Parameters regarding MTOW

Kellermann *et al.* (2020b)'s work presents a set of equations and graphs obtained for a set of 2000 aircraft, which allows the determination of some necessary parameters for the model. Among the variables of these models, Maximum Take-Off Weight (MTOW) stands out. Below are the coefficients and equations used in this work:

- Wing area: the total area of an aircraft ($A_{tot} [\text{m}^2]$) adheres to the following function:

$$\log_{10} A_{tot} = 0.748 \log_{10} MTOW - 0.689 \quad (22)$$

However, wings contribute only about 31% of this value. Furthermore, due to several components that need to be housed in the wing, the authors suggest that only 80% of the total area of a wing may be available to perform the function of a heat exchanger.

- Cooling requirement: considering the possible technologies that can be integrated into the aircraft, the authors suggest the following expression to estimate the required cooling power ($Q_{req} [\text{W}]$) due to the propulsion system, for the condition of take-off:

$$Q_{req} = (1 - \eta_{mec}) (1 - \eta_{he}) FVH_p \quad (23)$$

where $\eta_{mec} [-]$ is the mechanical efficiency, $\eta_{he} [-]$ is the electrical efficiency, $F [\text{N}]$ is the thrust force, $V [\text{m/s}]$ is the speed of the aircraft, and $H_p [-]$ is the degree of hybridization of the aircraft's power. In this work, it is assumed that this equation can be applied to all flight phases. In addition, to estimate thrust, the authors suggest the following expression:

$$\log_{10} F = 0.913 \log_{10} MTOW + 0.895 \quad (24)$$

In this work, the following coefficients were adopted, except when the text mentions another value: $\eta_{mec} = 0.50$, $\eta_{ele} = 0.90$, $H_p = 0.75$.

2.5.2 Surface temperature

To investigate the influence of the surface temperature of the wing on the ability to exchange heat through it, cases with the following temperatures will be evaluated: 300 K, 325 K, 350 K, and 400 K.

2.5.3 Aircraft Operation

Simulations will be carried out with the conditions presented in Tab. 2, in order to analyze the influence of speed and flight altitude on the performance of the heat exchanger.

Table 2: Phases of operation of an airplane.

Operation	Speed	Altitude
Take-off	69,0 m/s (250 km/h)	0 m (0 ft)
Climbing	125,0 m/s (450 km/h)	6.096 m (20.000 ft)
Cruise	236,0 m/s (850 km/h)	12.192 m (40.000 ft)

2.6 Cases of study: fuel integration

In order to obtain representative results for a commercial aircraft, part of the wing's geometric parameters were based on the Airbus A320, and are listed in Tab. 3. These values are used in the numerical model, except when another parameter is mentioned.

Table 3: Geometric and performance parameters of an A320.

Parameter	Value
Wingspan [m]	31,40 (Canada, 2019)
Mean aerodynamic chord [m]	4,19 (Agency, 2013)
MTOW [kg]	77.000 (GROUP, 2023)

2.6.1 Fuel flow

To investigate the influence of the fuel mass flow rate \dot{m}_f on the surface heat exchanger, simulations were carried out using the following flows: 1, 10, and 100 kg/s.

3. RESULTS

3.1 Wing study: Surface temperature and operation of the airplane

Figure 3 presents the results obtained for the heat removal capacity Q_{out} through the wing and the variation of the convection heat transfer coefficient h , considering initially different predetermined surface temperatures, altitude, and flow speeds. In these cases, the fuel flow under the wing's surface is not considered, and an exchange area of 200 m² is assumed.

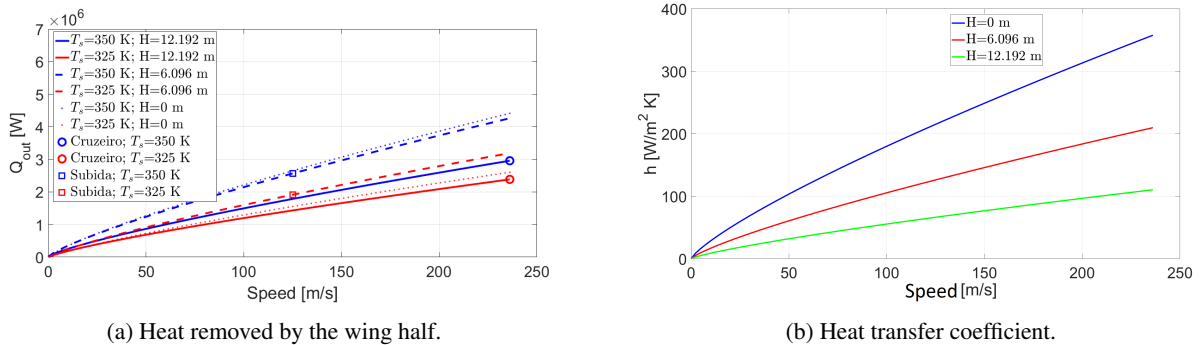


Figure 3: Wing performance.

The graph in Fig. 3a indicates that maximum heat transfer occurs at the lowest altitude, under the condition of maximum speed and surface temperature, achieving a transfer of 4.41×10^6 W. Next, the best condition occurs at an altitude of 6,096 m and results in 4.26×10^6 W. For all cases in Fig. 3a, it can be seen that low speeds result in low rates of heat transfer across the surface, while high velocities are related to the highest heat transfer rates. This result was already expected, as the convection heat transfer coefficient increases as the Nusselt number also increases (Fig. 3b). This, in turn, also increases when the flow velocity increases, a consequence of a higher Reynolds due to the higher velocity. In

addition, the surface temperature strongly impacts the results, with lower temperatures producing less heat exchange. This result was also expected since the temperature difference between the air and the wing's surface is smaller for $T_s = 325$ K than for $T_s = 350$ K.

In none of the evaluated scenarios did the best performance occur at maximum altitude, which may seem counterintuitive at first since it is in this condition that the atmospheric air temperature will be the lowest. However, when looking at the convective heat transfer coefficient in Fig. 3b, it can be seen that it decays significantly with altitude. Thus, knowing that the external forced convection is the main mechanism of heat transfer over the wing and that it depends on h and ΔT , the increase in the temperature difference between the surface and the air obtained with the temperature rise is counterbalanced by a decrease in the convective heat transfer coefficient, resulting in lower rates of heat at higher altitudes when traveling at a given speed. The decrease in air density with altitude is one of the parameters that most contribute to this scenario, as the Reynolds number depends on this parameter.

Therefore, although the graphs in Fig. 3a demonstrate the behavior for a wide range of speeds under different levels of altitude, it is worth noting that the operation of an aircraft presents a more restricted range of speeds for each stage of a flight, that is, in a low altitude condition, cruise flight speeds, which are the highest, are not used. As a result, in each curve, a possible combination of altitude and speed for the climb condition and cruise flight is highlighted, according to the data in Tab. 2. Therefore, considering the aircraft's possible operation, the markings in circles and squares represent the heat removal for when in cruise and climb flight, respectively. In these cases, the cruise condition always results in larger values for Q_{out} than the climb condition. Specifically for the purely turbulent regime, up to 2.96×10^6 W is removed in the cruise condition, while in the climbing, a peak of 2.57×10^6 W is reached.

3.2 Wing study: the dissipation of heat generated

Figure 4 presents results for heat dissipation under different temperatures for the wing surface, considering the take-off condition, that is, at sea level and a speed of 250 km/h. It is observed that the ability to remove heat increases significantly with surface temperature, reaching up to 1.6×10^7 W, as well as high MTOW improves this scenario. The positive dependence on MTOW can be explained by the fact that the wing area available for heat exchange increases with the increment of MTOW, as observed in Eq. 22. For this flight condition, Fig. 4b shows the ratio R_Q between the ability to remove heat (Q_{out}) and the amount of heat generated by the aircraft's propulsion system (Q_{req}). Values greater than unity for the fraction result mean that the wing could dissipate the heat generated by the aircraft. Therefore, in this case, except under the lowest temperature, the wing would have sufficient capacity to act as a surface heat exchanger, extracting the heat generated by the aircraft to all MTOW involved.

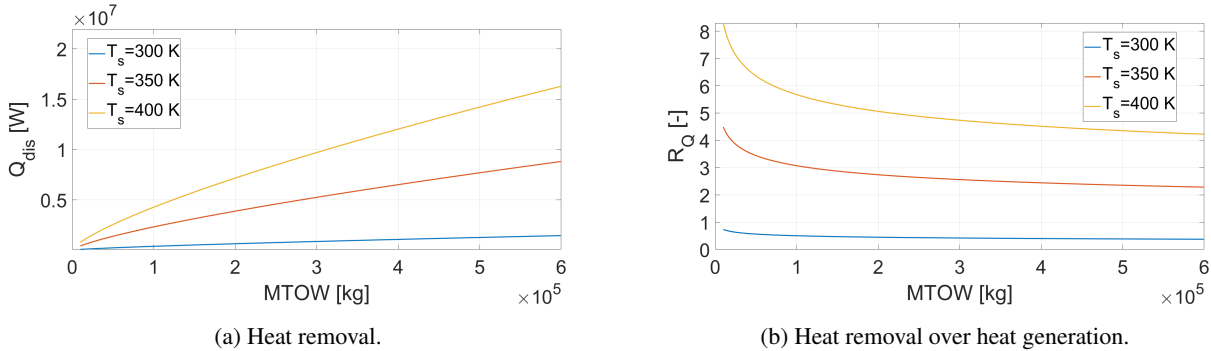


Figure 4: Wing performance for Takeoff condition.

The cruise condition is shown in Fig. 5. In this condition, there is an altitude of 40,000 ft and 850 km/h, and, as expected, it can dissipate more heat through the wing due to the higher speed involved and the lower temperature of the atmospheric air. However, the wing's potential to supply the necessary cooling for this condition is more limited, as seen in the R_Q levels of this scenario. Interestingly, for the lowest temperature, there is an increase in R_Q in relation to the previous case. These behaviors can be explained by the fact that the extracted and generated heat grows non-linearly with the speed and MTOW, specifically in the parameters Nu , A_{wing} , and F present in the calculations. Although the flow velocity has increased significantly and the air temperature has dropped, the maximum heat that can be extracted increases little from the previous scenario, reaching up to 2.3×10^7 W for the highest surface temperature. When the parameter Q_R is observed, it is noticed that the cruise flight has a lower capacity to remove heat compared to the demand for this condition.

In all cases (Fig. 4 and Fig. 5), it is observed that the use of the wing as a kind of surface heat exchanger is more favorable for low values of MTOW, that is, smaller aircraft. This same conclusion is observed in the work of (Kellermann *et al.*, 2020b). Although the operation at higher altitudes produces a scenario of greater heat extraction, mainly due to the speed involved, when taking into account the heat generation of the aircraft, the most attractive scenario becomes the one

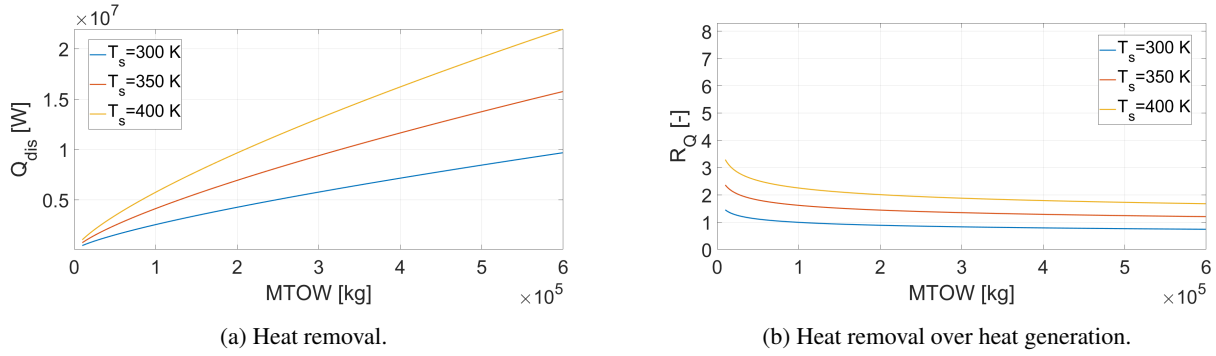


Figure 5: Wing performance for Cruise condition.

at lower altitudes, always with the higher surface temperature.

3.3 Fuel integration

The results to be discussed below contemplate different mass fuel flows, aircraft operations, and consider the parameters of the A320 aircraft.

Figure 6 illustrates the rate of heat dissipation along the span at each position (normalized by span) for takeoff and cruise conditions. As expected, in all cases, there is a reduction in the ability to remove heat along the span, a consequence of the decrease in fuel temperature as it advances through the span of the wing. In all cases, the fuel enters the wing with a temperature of 350 K. The Cruise condition has the highest heat removal rate due to a higher external speed and altitude, where greater cooling rates are observed. The highest fuel flows provide the best results when looking at the dissipated energy rate. The flow of 100.0 kg/s presents the highest levels of cooling, followed by the flow of 10.0 kg/s, and lastly, the flow of 1.0 kg/s. This trend is in line with Eq. 2, where it is shown that the dissipated energy Q_{out} is directly proportional to the mass flow \dot{m}_f .

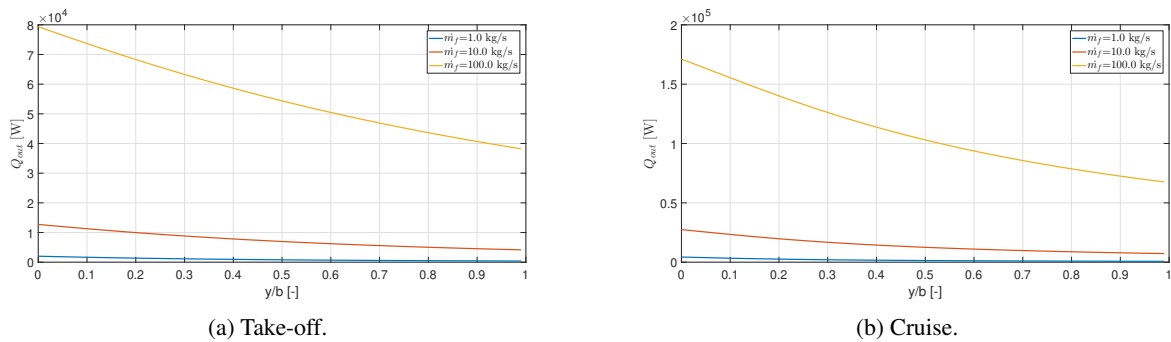


Figure 6: Heat removal along the span.

In both results of Fig. 6, the variation of Q_{out} is not linear. This can be explained due to the reduction in the temperature difference between the environment and the fuel along the span, and this reduction decreases the system's ability to exchange heat, generating this non-linear result.

4. CONCLUSIONS

The analyses carried out throughout the study demonstrated that the integration of a fuel duct responsible for transporting heat from other aircraft systems, under the surface of the wing, with the aim of exchanging heat with the external environment by convection, is plausible. Although the model adopts simplifying assumptions regarding the flow and geometry involved, such as a wing without tapering, sweeping, days without thermal variations, and steady and one-dimensional regime, the results allow exploring different scenarios that can be useful for the preliminary design of an aircraft.

The results obtained show that the exchanger's performance improves when the speed and altitude of the aircraft increase, as high heat values are extracted in this condition. However, considering the models adopted, heat generation by the aircraft also increases significantly with speed, resulting in a margin between the heat dissipation and heat generation ratio that is more comfortable at low speeds. The magnitude of the fuel flow under the wing is an important factor, and the results indicate that more attractive scenarios are obtained when high flows are applied, as expected.

Employing characteristics of the A320 aircraft, the modeling developed in this study suggests that the fuel-integrated

surface heat exchanger model is a promising technique, provided that certain altitude and fuel flow characteristics are met.

5. REFERENCES

- Agency, E.A.S., 2013. *EASA TYPE-CERTIFICATE DATA SHEET No. EASA.A.064*. European Aviation Safety Agency, 12th edition.
- Binns, C., 2018. *Aircraft Systems: Instruments, Communications, Navigation, and Control*. John Wiley & Sons.
- Bruno, T.J., 2008. "Thermodynamic, transport and chemical properties of "reference" jp-8".
- Canada, A., 2019. "Airbus a320-200 (320)". www.aircanada.com.br/aircanada/default.aspx?pageid=58, Accessed in 3rd May, 2023.
- Cengel, R.A., 2008. *Introduction to thermodynamics and heat transfer*. McGraw-Hill.
- Fortin, T.J. and Bruno, T.J., 2022. "Heat capacity measurements of conventional aviation fuels". *Fuel Processing Technology*, Vol. 235, p. 107341. ISSN 0378-3820. doi:<https://doi.org/10.1016/j.fuproc.2022.107341>. URL <https://www.sciencedirect.com/science/article/pii/S0378382022001813>.
- Gray, C. and Shayeson, M., 1973. "Aircraft fuel heat sink utilization. final technical report 14 apr 1972–14 apr 1973". Technical report, General Electric Co., Cincinnati, OH (USA). Aircraft Engine Technical Div.
- GROUP, L., 2023. "Airbus a320". <https://www.lufthansagroup.com/en/company/fleet/brussels-airlines/airbus-a320.html>, Accessed in June 1st, 2023.
- Kellermann, H., Habermann, A., Vratny, P. and Hornung, M., 2020a. "Assessment of fuel as alternative heat sink for future aircraft". *Applied Thermal Engineering*, Vol. 170, p. 114985.
- Kellermann, H., Habermann, A.L. and Hornung, M., 2020b. "Assessment of aircraft surface heat exchanger potential". *Aerospace*, Vol. 7, No. 1. ISSN 2226-4310. doi:10.3390/aerospace7010001. URL <https://www.mdpi.com/2226-4310/7/1/1>.
- Roland, J. and Rumpfkeil, M.P., 2017. "Wing fuel-tank heat-sink calculation for conceptual aircraft design". *Journal of Aircraft*, Vol. 54, No. 3, pp. 1172–1188.
- Rosero, J., Ortega, J., Aldabas, E. and Romeral, L., 2007. "Moving towards a more electric aircraft". *IEEE Aerospace and Electronic Systems Magazine*, Vol. 22, No. 3, pp. 3–9. doi:10.1109/MAES.2007.340500.
- Sadraey, M., 2017. *Aircraft Performance: An Engineering Approach*. CRC Press. ISBN 9781523117949. URL <https://books.google.com.br/books?id=0aelwgEACAAJ>.
- Schlabe, D. and Lienig, J., 2016. "Model-based thermal management functions for aircraft systems". *Aircraft Thermal Management: Integrated Energy Systems Analysis*, Vol. 178, p. 89.
- van Heerden, A.S., Judt, D.M., Jafari, S., Lawson, C.P., Nikolaidis, T. and Bosak, D., 2022. "Aircraft thermal management: Practices, technology, system architectures, future challenges, and opportunities". *Progress in Aerospace Sciences*, Vol. 128, p. 100767.

6. RESPONSIBILITY NOTICE

The authors are solely responsible for the printed material included in this paper.